performed in the years 1985 to 1987. Reinhold Kühl

Makromol. Chem., Macromol. Symp. **17**, 1–16 (1988)

RECOGNITION HYSTERESIS OF THE ACETYLCHOLINE RECEPTOR OF TORPEDO CALIFORNICA

Reinhold Kühl et al Rheinstr. April 22, 200

Eberhard Neumann, Elvira Boldt, Barbara Rauer, Hendrik Wolf and Hai Won Chang*

Faculty of Chemistry, University of Bielefeld, P.O.Box 8640, D-4800 Bielefeld 1, F.R.Germany, *Department of Neurology, College of Physicians and Surgeons, Columbia University, New York, N.Y. 10032,U.S.A.

Abstract: The nicotinic acetylcholine receptor (nAcChR) of the electric organ of Torpedo californica fish exhibits a pronounced hysteresis loop in the high affinity binding of the neurotransmitter acetylcholine (AcCh). When increasing amounts of AcCh are added (pulse mode) an extremely long-lived, metastable conformer distribution is obtained (lower hysteresis branch) between low affinity AcCh binding states (R_l) and high (R_h) and very high (R_{vh}) affinity states. Dialysis conditions always lead to the equilibrium binding curve (upper hysteresis branch; $\bar{K}_A = 5 \times 10^{-9}$M, 4°C; one A bound to the R-monomer of $M_r \approx 290\,000$). Cyclic, pulse mode addition and dilution of AcCh results in scanning loops within the main hysteresis.
The kinetic analysis of the changes in free and bound AcCh during the open-system conditions of dialysis, that releases the metastability, shows that the AcCh (A) binding proceeds along an induced-fit pathway according to $A+R_h \rightleftharpoons AR_h \rightleftharpoons AR_{vh}$. The rate constant of the step $AR_h \rightarrow AR_{vh}$ is $k_2 = 6 \times 10^{-3} s^{-1}$ and that of the reverse step is $k_{-2} = 3 \times 10^{-4} s^{-1}$. Direct binding of A to free R_{vh} can be excluded. Therefore, the state R_{vh} does not preexist, it is induced and only stable, as AR_{vh}, by bound AcCh. The metastability can be described in terms of long-lived $AR_{vh} \cdot R_l$ hybrid dimers.
Physiologically, the metastable hybrid may be viewed as a saving device: the functionally important, channel-active R_l conformer is, at low AcCh-concentrations [A] < 1μM, prevented to convert to the desensitized states R_h and AR_{vh}. Furtheron, AcCh enhances the phosphorylation of phosphatidyl inositol and the auto-phosphorylation of the receptor. If the AcCh binding hysteresis causes a phosphorylation hysteresis the desensitized nAcChR may serve as a memory molecule of the transsynaptic information signalling of the neurotransmission.

INTRODUCTION

The binding of a neurotransmitter molecule to its receptor macromolecule (1) may be viewed as molecular recognition if the functional specificity, relative to competitive ligand molecules, justifies the anthropomorphic term recognition (2). In the case of the neurotransmitter acetylcholine (AcCh) the binding to the nicotinic acetylcholine receptor (nAcChR) of Torpedo electric organ is associated with a pronounced hysteresis loop (1)

This phenomenon may thus be termed recognition hysteresis.

In synaptic nerve-nerve and nerve-muscle contact sites, AcCh and the cholinergic protein system are the mediator of the electrical-chemical information flux across the synapses. Neurophysiologically, AcCh is essential for memory; deficiency of AcCh causes memory loss (3,4). On the other hand, memory imprint and recognition memory are believed to be based on the strength of a synapse. Now, since hysteresis is a physical mechanism for memory imprint (5-7) it is tempting to associate a synaptic acetylcholine recognition hysteresis with elements of the synaptic recognition memory of sensory perceptions.

In physical chemistry hysteresis is an indicator of cooperativity on the nonequilibrium level of domain structures (8). Functionally, hysteresis is not only a mechanism for physical memory recording but also for chemical oscillations (5).

The structural concept of nonequilibrium cooperativity and long-lived metastability can be successfully applied to the analysis of the acetylcholine recognition hysteresis; see Fig. 1 (9).

Here, the binding hysteresis is obtained when membrane fragments rich in the nicotinic acetylcholine receptor (nAcChR) are just mixed with AcCh of increasing concentration (pulse mode addition of AcCh) up to [A] ≈ 1 μM, yielding the lower branch, followed by a gradual dilution of AcCh resulting in the upper branch of the hysteresis loop. If, however, the AcCh binding is studied under the open system conditions afforded by equilibrium dialysis, a concentration-dilution cycle always traces the upper curve. Although the binding of the pulse mode addition is time independent ($\geq$ 17h, 4°C), it is only the upper curve that reflects true equilibrium binding (1).

Because the rapid, pulse-like addition of AcCh to the nAcChR leads to less binding, receptor binding sites R_l of lower affinity are preserved. Indeed it is known that in the range of the acetylcholine concentration [A] $\leq$ 1 μM where hysteresis is observed only the high-affinity receptor conformers and not the low-affinity ones of the conformational equilibria ($R_l \rightleftharpoons R_h$) are the targets of AcCh binding. Obviously, the extent to which the conformational equilibria are shifted to the side of the high-affinity conformers is dependent on the mode of increasing the acetylcholine concentration (simple mixing versus dialysis).

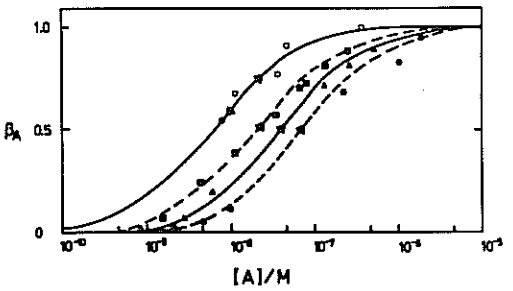

Fig. 1. Recognition hysteresis of high-affinity acetylcholine binding to T.cal. nAcChR in membrane fragments at 4°C: ○, equilibrium dialysis data of [^{3}H]AcCh binding, [R_T] = 0.4 μM; the curve is calculated using $\beta_A = [A]/([A] + \bar{K})$ with $\bar{K} = (5 \pm 1) \times 10^{-9}$M; ■, ▲, ●, pulse mode addition (mixing) of [^{3}H]AcCh at [R_T]= 0.1, 0.4 and 1.0 μM total receptor concentrations, respectively, (α-Btx sites in the absence of detergent). The data are corrected for radioimpurity, acetylcholinesterase activity and non [^{3}H]AcCh radioactivity (9).

In the present study the existence of scanning curves (8) is shown; the kinetics of AcCh binding under dialysis conditions (10) and the detergent-induced binding of a second α-bungarotoxin molecule (1,11,12) to the nAcChR in membrane fragments are analyzed. The main result is that the final very high affinity conformer R_{vh} does not preexist in its unliganded form. Rather, it is induced by AcCh binding and is only stable as the acetylcholine binding complex AR_{vh}.

MATERIALS AND METHODS

The method of preparing AcChR-rich membrane fragments from Torpedo californica electric organ was that of Sobel et al. (13) with some modifications (1). The total nAcChR concentration [R_T] was dermined by the number of ^{125}I-α-bungarotoxin (α-Btx) sites measured by the DE-81 (Whatman) filter disk method (14); see also Ref. 1. Acetylcholinesterase activity of the membrane fragments was assayed by the Ellman test; the enzyme was blocked as described in ref. (1). In the pulse mode addition of AcCh the binding of [^{3}H]AcCh was measured by the ultracentrifugation

method. Bound and free AcCh were determined directly. Radiochemical purity of [^{3}H]AcCh was determined by TLC.*) The [^{3}H]AcCh concentration was corrected for residual esterase activity and non [^{3}H]AcCh contributions (1). (*) thin layer chromatography)

In the dialysis mode the concentration of free [^{3}H]AcCh inside the dialysis bag changes with time; it had to be determined directly from the bag contents.

RESULTS

Detergent effect on α-bungarotoxin binding

The binding of α-Btx is a well established method to quantitatively determine nAcChR binding sites. Recently it has been discovered that when membrane fragments are exposed to 0.1 % (≈ 2 mM) Triton X100 they bind twice as much α-Btx compared to the absence of the detergent. Fig. 2 shows that increasing amounts of Triton X100 cause a gradual increase in the binding of a second α-Btx molecule per monomer (M_r=290 000) of the receptor dimer R·R. The titration with Lubrol WX leads to a similar binding curve.

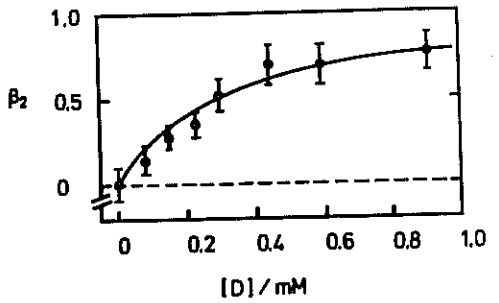

Fig. 2. The degree β_2 of the binding of the second α-Btx molecule to the nAcChR of T.cal. membrane fragments as a function of Triton X100 concentration [D] at 4°C, 30 mM NaCl, 1 mM $CaCl_2$, 4 mM KCl, 4 mM Na-phosphate, 1 mM Pipes, 0.05 mM EDTA, 0.3 mM NaN_3, pH 7, Initial (at [D] = 0) concentrations of AcChR in terms of M_r = 290 000, $[R_T]$ = 0.03 μM, of α-Btx [B] = 0.24 μM; equilibrium constants of α-Btx binding: $K_1 \approx K_2 = 10^{-11}$M. Pipes = piperazine-N,N'-bis(2-ethanesulfonic acid);

Scanning curves

The hysteresis loops in Fig. 1 appear to increase in size with increasing receptor concentration. Since the scatter of the [^{3}H]AcCh data points is, however, rather large, the present accuracy of the method is not sufficient to argue in terms of a concentration dependence. The half-binding distribution constant Q of the receptor concentration range $[R_T]$ = 0.4 - 1.0 μM is Q = (4 ± 2) x 10^{-8}M; the equilibrium constant is $\bar{K}$ = 5 x 10^{-9}M as in Ref. 1.

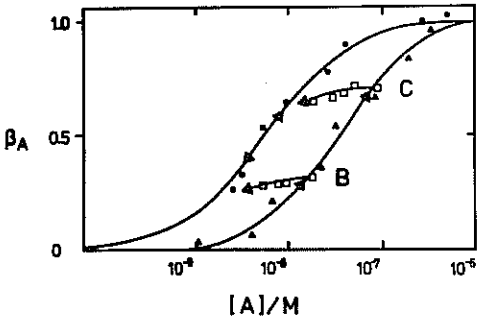

Fig. 3. Scanning curves of the nAcChR of T.cal. membrane fragments. Main hysteresis loop of pulse-like addition of AcCh (▲ , →) and of dilution from [A] > 1 μM along the equilibrium (dialysis) curve (● , ↔). □, dilution curves starting from the lower hysteresis branch. $[R_T]$ = 1 μM, $\bar{K}$ = 5 x 10^{-9}M and Q ≈ 4 x 10^{-8}M. See Fig.1.

Fig. 3 exhibits scanning curves within the main hysteresis loops. For instance, AcCh was added to membrane fragments to obtain β_A = 0.3 at [A] = 4 x 10^{-8}M, point B on the pulse mode binding curve (lower hysteresis branch). Subsequently the AcCh concentration was decreased by dilution. If the pulse mode binding curve were an equilibrium curve the dilution would trace this curve backward. Instead the dilution curve enters as a scanning curve into the main hysteresis loop. The same is true for the dilution curve starting at point C.

Kinetics of [^{3}H]AcCh binding in dialysis mode (10)

Fig. 4 shows the time courses of the concentrations of free [^{3}H]AcCh, $[A]_{in}$, and of the bound [^{3}H]AcCh, $[A_b]$, both inside the dialysis bag. [^{3}H]AcCh was added to membrane fragments in the bag (pulse mode, yielding an initial value of β_o and of $[A_o]_{in}$ on the lower hysteresis branch. At time zero the bag was exposed to dialysis conditions.

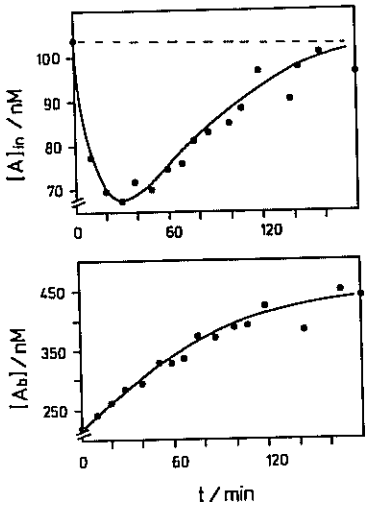

Fig. 4. Kinetics of the dialysis mode [^{3}H]AcCh binding. Upper part: Change in the [^{3}H]AcCh concentration $[A]_{in}$ of membrane fragments / [^{3}H]AcCh solution prepared by the pulse mode, inside the dialysis bag as a function of dialysis time. At the start of the dialysis at t = 0, $[A]_{in} = [A_o]$ and $\beta_A = \beta_o$. Lower part: Time course of additional [^{3}H]AcCh binding caused by the dialysis. Dashed line: $[A]_{out}$ in the absence of AcChR.

It is seen that, surprisingly, $[A]_{in}$ first decreases and then increases to the level $[A]_{out}$, the [^{3}H]AcCh concentration outside the bag. The bound AcCh gradually increases until the equilibrium value on the upper hysteresis branch is reached. It appears that in the initial phase the additional binding of AcCh is faster than the diffusional supply of AcCh from the outside solution such that $[A]_{in}$ sinks below the level $[A]_{out}$. The characteristic behaviour of $[A]_{in}$ and $[A_b]$ is intrinsic to the open systems condition of the dialysis.

DISCUSSION

Detergent binding to nAcChR

The data in Fig. 2 suggest that detergent binding causes changes in the membrane bound nAcChR that permit the binding of a second α-Btx molecule. The data can be described in terms of the steric hindrance model for the second α-subunit of the monomer ($M_r \approx 290\,000$). It appears that increasing concentration of the detergent releases the hindrance such that the second α-site is also occupied by α-Btx (12).

Whereas in the absence of detergents (D) the binding of α-Btx (B) to the receptor monomer (R) is globally described by

$$B + R \overset{(K_1)}{\rightleftharpoons} BR, \qquad (1)$$

the reaction sequence for the D titration in the presence of an excess of B is given by:

$$nD + BR \overset{(K_D)}{\rightleftharpoons} \ldots \rightleftharpoons BR{\cdot}D_{n-1} + D \overset{(K_D)}{\rightleftharpoons} BR{\cdot}D_n \qquad (2)$$

$$BR{\cdot}D_n \overset{(K_c)}{\rightleftharpoons} BR'{\cdot}D_n$$

$$B + BR'{\cdot}D_n \overset{(K_2)}{\rightleftharpoons} B_2R'{\cdot}D_n \qquad (3)$$

The structural transition $R \rightleftharpoons R'$ converts the second α-site to a conformation that binds α-Btx with high affinity as soon as n detergent molecules have bound. Because of the high-affinity binding of the second B the smooth curve in Fig. 2 indicates the independent and allosteric nature of the detergent binding. The reaction (3) does apparently not shift the reaction (2) which is only dependent on the concentration of D. The reaction (3) may be used to measure the detergent effect on the receptor. Therefore the degree of the binding of the second α-Btx, $\beta_2 = [B_2R'{\cdot}D_n]/[R_T]$ relative to the total receptor concentration $[R_T]$, can be related to [D] by (11,12):

$$\beta_2 = \frac{K_c}{1 + K_c} \cdot \frac{[D]}{\bar{K}_D + [D]} \qquad (4)$$

where $\bar{K}_D = K_D/(1 + K_c)$ is the overall detergent equilibrium dissociation constant. For D = Triton X100, we obtain at 4°C and

the conditions given in the legend of Fig. 2: $\bar{K}_D = 2.8\ (\pm\ 0.3) \times 10^{-4}$M. For the detergent Lubrol WX we obtain $\bar{K}_D = 3.3\ (\pm\ 0.4) \times 10^{-4}$M. These constants are apparent quantities partially reflecting lipid-detergent exchange of the receptor protein.

Domain structure of nAcChR in membrane fragments

The AcCh binding hysteresis and the existence of scanning curves, see Fig. 3, qualify the nAcChR as a physical memory molecule with cooperative nonequilibrium domain structure (7,8). The scanning curves are additional evidence for the previous conclusion that the pulse mode addition of AcCh to nAcChR membrane fragments does not yield equilibrium values for β_A and [A]. Rather, at the level of high affinity AcCh binding at [A] ≤ 1 μM simple (non-dialytic) mixing of nAcChR with AcCh leads to nonequilibrium distributions of low- and high-affinity conformers. The nonequilibrium distribution is extremely long-lived, it may be characterized by a half-binding constant Q. However, any equilibrium analysis of pulse mode data in terms of equilibrium binding cooperativity (upward curvature of Scatchard plots) is forbidden. Already the fact that only one AcCh binds to the high-affinity receptor conformer in equilibrium excludes any ligand-binding cooperativity.

The nonequilibrium cooperativity indicated by hysteresis and scanning (8) can be successfully analyzed in terms of the receptor dimer concept (1,12,15). In particular the notion of a dimer hybrid $R_l \cdot R_h$ has proven to be very useful.

It is known that also in the absence of AcCh binding a conformational equilibrium of the type $R_l \rightleftharpoons R_h$ exists between low-affinity (R_l) and high-affinity (R_h) conformers. The data suggest that the equilibrium constant K_h of AcCh binding to R_h has a value of about 10^{-7}M. Therefore R_h is a conformer of intermediate affinity for AcCh; it is not the final conformer of highest affinity. The data in Fig. 4 suggest that the final receptor conformer, leading to the overall value $\bar{K} = 5 \times 10^{-9}$M at 4°C is only stable in the AcCh binding form AR_{vh}.

Analysis of the [^{3}H]AcCh dialysis kinetics

Cyclic reaction scheme. The kinetic analysis of the dialysis data in Fig. 4 requires a reaction scheme involving R_l ($K_l \approx 10^{-4}$M), R_h ($K_h \approx 10^{-7}$M) and R_{vh} ($K_{vh} \ll \bar{K}$). At AcCh concentrations [A] < 1 μM, the AcCh binding to R_l can be neglected (< 1%); hence the minimum reaction scheme for the binding of AcCh in terms of the monomer units R reads:

$$\begin{array}{ccccc} & & R_l & & \\ & & \Big\uparrow\downarrow\ (K_{l,h}) & & \\ & & \overset{(K_l)}{\rightleftharpoons} & & \\ A + R_h & & & & AR_h \\ & & \Big\uparrow\downarrow\ (K_o) & & \Big\uparrow\downarrow\ (K_2) \\ & & \underset{(K_3)}{\rightleftharpoons} & & \\ A + R_{vh} & & & & AR_{vh} \end{array} \qquad (5)$$

The induced-fit model. In scheme (5) the final high-affinity complex AR_{vh} can be obtained along two limiting pathways. The kinetic analysis will show that only the induced fit-pathway

$$\begin{array}{ccccc} & & R_l & & \\ & & \Big\uparrow\downarrow & & \\ A + R_h & & \overset{(K_l)}{\rightleftharpoons} & & AR_h \\ & & & & \Big\uparrow\downarrow\ k_2 \\ & & & & k_{-2} \\ & & & & AR_{vh} \end{array} \qquad (6)$$

is consistent with the data. The pathway of direct, selective binding of A to the conformer R_{vh} is negligible, i.e. practically excluded.

The practical, apparent equilibrium constant for the high-affinity AcCh binding for the general scheme (5) is given by

$$\bar{K} = \frac{[A]([R_h] + [R_{vh}])}{[AR_h] + [AR_{vh}]} = \frac{K_l\ (\ 1 + K_o^{-1})}{1 + K_2^{-1}} \qquad (7)$$

where the individual equilibrium and rate constants are given by:

$$K_1 = [A][R_h]/[AR_h] \quad (8)$$

$$K_2 = [AR_h]/[AR_{vh}] = k_{-2}/k_2$$

$$K_3 = [A][R_{vh}]/[AR_{vh}]$$

$$K_o = [R_h]/[R_{vh}] = k_{-o}/k_o$$

$$K_{1,h} = [R_l]/[R_h]$$

For the induced fit model in scheme (6), eq. (7) is reduced to

$$\bar{K} = K_1 / (1 + K_2^{-1}) = K_1K_2/(1 + K_2) \quad (9)$$

Rate equation. The fundamental rate equation for the slow increase in the concentration of the complex AR_{vh} (observed in Fig. 4) is:

$$d[AR_{vh}]/dt = k_2[AR_h] - k_{-2}[AR_{vh}] \quad (10)$$

The degree of total high affinity binding is defined by $\beta = [A_b]/[R_T]$ or explicitly:

$$\beta = ([AR_{vh}] + [AR_h])/[R_T] = [AR_{vh}](1 + K_2)/[R_T], \quad (11)$$

where mass conservation implies that the total receptor (binding site) concentration is:

$$[R_T] = [R_h] + [R_l] + [AR_h] + [AR_{vh}] \quad (12)$$
$$= [R_h](1 + K_{1,h}) + \beta\cdot[R_T]$$

Because of the hour-kinetics indicated in Fig. 4 it is reasonable to assume that the bimolecular binding step (associated with K_1) is fast compared to the slow structural transition (k_2, k_{-2}). Therefore, $[AR_h]$ is given by the pre-equilibrium:

$$[AR_h] = K_1^{-1}\,[A][R_h] \quad (13)$$

Eq. (12) yields $[R_h] = (1-\beta)[R_T]/(1 + K_{1,h})$, substitution into eq. (13) and furtheron into eq. (10) finally leads to the practical rate equation:

$$d\beta/dt = a\cdot[A](1-\beta) - k_{-2}\cdot\beta \quad (14)$$

where with eqs. (8) and (9):

$$a = k_2(1+K_2)/[K_1(1+K_{1,h})] = k_{-2}/[\bar{K}(1+K_{1,h})] \quad (15)$$

Initial rate. It is readily seen that

$$d\beta/dt = -d(1 - \beta)/dt = -(d[A]/dt)/[R_T] \quad (16)$$

At the start of the dialysis at $t = 0$, $\beta = \beta_o$ and $[A]_{in} = [A_o]$, inside the dialysis bag. Because $\bar{K}^{-1} \gg 1$, the initial rate of [^{3}H]AcCh binding at $t = 0$ is given by

$$(d\beta/dt)_o = a\cdot[A_o](1 - \beta_o) \quad (17)$$

or, from eq. (16):

$$(d[A]/dt)_o = -a(1-\beta_o)[R_T]\cdot[A_o] \quad (18)$$

Lumping the experimental quantities together we may define a relative initial rate:

$$v_o = -(d[A]/dt)_o/[(1 - \beta_o)[R_T]] = a[A_o] \quad (19)$$

It is seen from eqs. (18) and (19) that the induced-fit model in scheme (5) predicts that the initial rate of the decrease in $[A]_{in}$ is proportional to the initial AcCh concentration at the start of the dialysis.

On the other hand the limiting case of rapid direct, selective binding $A + R_{vh} \rightleftharpoons AR_{vh}$ coupled to the slow, rate-determining step $R_{vh} \rightleftharpoons R_h$; k_{-o}, k_o) leads to an expression for the initial relative rate

$$v_o = -(d[A]/dt)_o/[(1 -\beta_o)[R_T]] = k_o \quad (20)$$

being a constant, independent of $[A_o]$. The analysis of the dialysis data according to eq. (19) is rather inaccurate because of the inaccuracy of graphical slope determinations. However, Fig. 5 shows that the v_o-values are dependent on $[A_o]$. The linear approximation yields $a \approx 3 \times 10^{-4}\,nM^{-1}min^{-1}$.

Integral rate equation. Since, however, a set of two data, [A]and $\beta = \beta_A$, are available for every time point, the entire time courses may be analytically treated. For this purpose eq. (14) is rewritten as

$$d\beta/dt = a[A] - a([A] + \bar{K})\beta \quad (21)$$

Eq. (21) is an inhomogeneous differential equation, solved by first solving the homogeneous form $d\beta/dt = -a([A] + \bar{K})\beta$ yielding $\beta = C\cdot\exp[-a\int([A] + \bar{K})dt]$, where C is

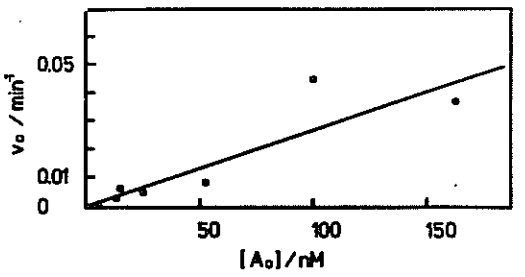

Fig. 5. Dependence of the initial relative rate v_o on the initial AcCh concentration $[A_o]$ in the dialysis bag, see eq. (19) of the text.

By the method of variation of C we obtain, within the integration boundaries t and $t_o = 0$, β and $\beta(t = 0) = \beta_o$, the integral form:

$$\beta = (\beta_o + a\int[A]\exp[a\int([A] + \bar{K})dt]dt)\exp[-a\int([A] + \bar{K})dt] \qquad (22)$$

The available data base permits a graphical evaluation replacing the integrals by sums according to

$$\int_o^t [A(t)]dt = \Sigma_{i=1}[\bar{A}_i]\Delta t_i \qquad (23)$$

where $[\bar{A}_i] = ([A]_i + [A]_{i-1})/2$

and $\Delta t_i = t_i - t_{i-1}$ with $t_{i-1} = t_o$ at $i = 1$.

Introducing the terms

$$y = \beta - \beta_o \cdot b \qquad (24)$$

$$x = (\Sigma[\bar{A}_i]\exp[a\,\Sigma([\bar{A}_j] + \bar{K})\Delta t_j]_i \cdot \Delta t_i) \cdot b \qquad (25)$$

$$b = \exp[-a\Sigma([\bar{A}_i] + \bar{K})\Delta t_i]$$

the dialysis data can be evaluated according to $y = a \cdot x$. As shown in Fig. 6 the dependence is linear yielding $a = 6.5 \times 10^{-4}\,nM^{-1}min^{-1}$.

The fraction of R_l conformers (at [A] = 0) was estimated ≈ 0.8 (Ref. 16); thus $K_{l,h} = 0.8/0.2 = 4$. From eq. (15) we obtain $k_{-2} = a\,\bar{K}(1 + K_{l,h}) = (2.7 \pm 0.2) \times 10^{-4}s^{-1}$. Since $[AR_{vh}]$ appears to be large compared to $[AR_h]$, $K_2^{-1} \ll 1$;

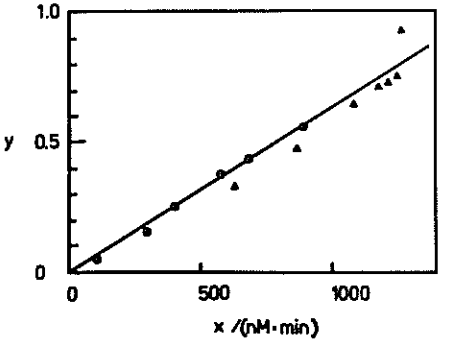

Fig. 6. Dialysis data evaluation according to y = ax derived from eq. (22) of the text; ●, ▲, $[A_o] = 14.6$nM, 104 nM.

therefore $\bar{K} \approx K_1K_2 \approx K_1 \cdot k_{-2}/k_2$. If we take the estimate $K_1 \approx 10^{-7}$M, we find $k_2 \approx K_1k_{-2}/\bar{K} \approx 5.4 \times 10^{-3}s^{-1}$ and $K_2 \approx 0.05$. The numerical values of $k_2 \approx 5.4 \times 10^{-3}s^{-1}$ and of $k_{-2} \approx 0.27 \times 10^{-3}s^{-1}$ correspond to the rather slow kinetics of the additional AcCh binding under dialysis conditions. The intrinsic relaxation rate of the $AR_h \rightleftharpoons AR_{vh}$ equilibration is given by $1/\tau = k_2 + k_{-2} \approx 5.67 \times 10^{-3}s^{-1}$ or $\tau \approx 3$min. This value may be compared to the time constant of AcCh equilibration across the dialysis bag in the absence of binding (no membrane fragments): $\tau_{eq} \approx 30$ min. Therefore the kinetics of [A]-changes in the presence of membrane fragments must be rate-limited by the receptor structural changes. The rather dramatic decrease of $[A]_{in}$ within about 30 min after start of the dialysis is caused by the rather limited size of the surface of the dialysis bag limiting the net amount of AcCh which can enter the bag. In the initial dialysis phase the nAcChR-rich membrane fragments bind more AcCh than can be supplied by diffusion from the outside of the dialysis bag.

Reaction scheme of the AcCh recognition hysteresis. On the basis of the kinetic data (10) the reaction scheme previously developed to rationalize thermodynamic data (1) can be specified in terms of the induced fit mechanism, excluding direct binding of AcCh to the very high affinity conformer

because its concentration is negligibly small. See Fig. 7.

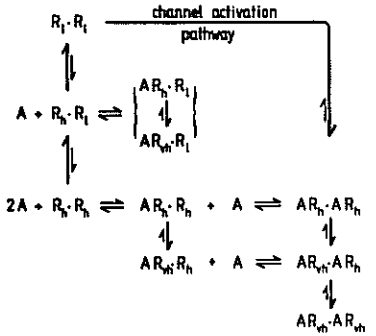

Fig. 7. Reaction scheme of AcCh binding to AcChR to account for the difference in AcCh-binding profile resulting from "single-pulse mode addition" (closed system with respect to AcCh) and "dialysis mode addition" open system). The simple bimolecular processes are represented by the horizontal sequences, whereas the vertical steps model the various slow structural isomerizations. R_l: low-affinity conformer $K_l \approx 10^{-4}$M; R_h: high-affinity conformer ($K_h \approx 10^{-7}$M; R_{vh}: very high affinity conformer ($K_{vh} \ll \bar{K} \approx (5\pm1)\times 10^{-9}$); $R_h \cdot R_l$: hybrid form of the two binding sites. The thick arrows indicate the preferential position of the isomerization equilibria. Large upper arrow indicates the channel activation pathway. At high AcCh concentration (>10^{-6}M), the low-affinity conformer, R_l, is directly involved in the binding which results in channel opening and, at prolonged exposure to AcCh, is subsequently transformed to the high-affinity conformers. At low AcCh concentrations (<10^{-6}M), the R_h(and R_{vh}) conformer is the dominant direct reaction partner for AcCh and thus constitutes the direct route of the high affinity state pathway to the final complex AR_{vh}. "Single pulse mode addition" of AcCh (closed system) favors the hybrid $AR_{vh} \cdot R_l$ binding state, whereas "dialysis mode addition" (open system) ultimately leads to the $AR_{vh} \cdot AR_{vh}$ conformer.

Physiological aspects of the AcCh recognition hysteresis

In cholinergic synapses the nAcChR is at a strategically important position of the postsynaptic membrane. According to the present concept the nerve impulse leads to release of AcCh (17). The AcCh cation binds to (recognizes) the nAcChR membrane receptor and causes a transient structural change (18) to the open channel conformation of this Na^+/K^+ transport-gating protein.

The transient cation flux causes membrane depolarization which finally may trigger impulses in the subsynaptic cell membrane.

The open channel conformation of the nAcChR protein is short-lived metastable (19). In the prolonged presence of AcCh the active channel-open phase converts to inactive, desensitized receptor conformers of high and very high affinity for AcCh (20). It is only the R_l conformers which are involved in channel activity, most likely as highly cooperative dimers (double-channels) as shown recently (15). However, due to the conformational coupling ($R_l \rightleftharpoons R_h$) the low-affinity receptor conformers are also affected by the hysteresis of the high-affinity conformers.

In any case the metastable hybrid conformations $AR_h \cdot R_l$, $AR_{vh} \cdot R_l$ may be viewed as a saving device for the functionally important, channel active R_l conformers. At low AcCh concentrations, [A] < 1 μM, hysteresis comprises a mechanism to prevent the total conversion to the inactivated, desensitized conformers. It has been recently shown (Kiehl, Varsanyi and Neumann, 1987) that AcCh binding enhances the phosphorylation of phosphatidylinositol by the isolated nAcChR/lipid complex and the autophosphorylation of the receptor. If now the AcCh-binding hysteresis is concomitant with a phosphorylation hysteresis, the (desensitized) nAcChR may serve as a memory molecule in the transsynaptic information flux of nerve-nerve and nerve-muscle synapses. Thus,the AcCh recognition hysteresis may be a part of the molecular mechanism of synaptic memory imprint and recognition memory.

ACKNOWLEDGEMENTS

We thank M. Pohlmann for the typing of the manuscript and the Deutsche Forschungsgemeinschaft for financial support, grant D 3, SFB223, to E.N; grant NS-1/766 to H.W.Ch.

REFERENCES

(1) H.W. Chang, E. Bock and E. Neumann, Biochemistry, 23, 4546-4556 (1984).
(2) E. Neumann, Comments Mol. Cell. Biophys., 4, 121-141 (1987)
(3) E.A. Murray and M. Mishkin, Science, 228, 604-606 (1985)
(4) M. Mishkin and T. Appenzeller, Scient. Amer., 62-71 (1987)

(5) A. Katchalsky and R. Spangler, Quart. Rev. Biophys., 1, 127-175 (1968)

(6) A. Katchalsky and E. Neumann, Int. J. Neurosci., 3, 175-182 (1972)

(7) E. Neumann, Angew. Chem., 85, 430-444 (1973); Int.Ed.Engl. 12, 356-369 (1973).

(8) D.H. Everett, Trans. Faraday Soc., 51, 1551-1557 (1955)

(9) H. Wolf, Diploma thesis, University of Bielefeld (1986).

(10) B. Rauer, Diploma thesis, University of Bielefeld (1987)

(11) E. Boldt, Diploma thesis, University of Bielefeld (1986)

(12) E. Neumann, in: Nicotinic Acetylcholine Receptor, ed. A. Maelicke, NATO ASI Series, Vol. H3, 177-196 (1986)

(13) A. Sobel, M. Weber and J.P. Changeux, Eur.J.Biochem., 55, 505-515 (1975)

(14) H.W. Chang and E. Bock, Biochemistry, 16, 4513-4520 (1977)

(15) H. Schindler, F. Spillecke and E. Neumann, Proc. Natl. Acad. Sci. USA, 81, 6222-6226 (1984)

(16) N.D. Boyd and J.B. Cohen, Biochemistry, 19, 5344-5353 (1980)

(17) B. Katz, The release of neural transmitter substances, Liverpool Univ. Press, Liverpool, U.K. (1969), p. 55.

(18) D. Nachmansohn, The Harvey Lect., 49, 57-99 (1955)

(19) E. Neumann and J. Bernhardt, J. Physiol. (Paris) 77, 1061-1072 (1981)

(20) B. Sakmann, J. Patlak and E. Neher, Nature, 286, 71-73 (1980)

Theses (9)–(11) by R. Kiehl 1985–1987

Address of correspondence: E. Neumann, Bielefeld.